



## Research Paper

## Insights from a shallow foundation load-settlement prediction exercise

J.P. Doherty<sup>a,\*</sup>, S. Gourvenec<sup>b</sup>, F.M. Gaone<sup>b</sup><sup>a</sup> School of Civil, Environmental and Mining Engineering, The University of Western Australia, 35 Stirling Hwy, Crawley, WA 6009, Australia<sup>b</sup> Centre for Offshore Foundation Systems and the ARC Centre of Excellence for Geotechnical Science and Engineering, The University of Western Australia, Crawley, WA, Australia

## ARTICLE INFO

## Keywords:

Shallow foundation  
Soft clay  
Field tests  
Prediction exercise

## ABSTRACT

This paper describes an international exercise aimed at assessing the geotechnical engineering profession's ability to predict the response of shallow foundations on soft clay subjected to undrained loading. Predictions of bearing capacity varied by more than an order of magnitude and settlement by more than two orders of magnitude. Average and median predicted values deviated significantly from measured values. The results of this exercise highlight the need to develop tools to assist engineers to process site investigation data. The development of predictive models that connect directly to site investigation data is discussed.

© 2017 Elsevier Ltd. All rights reserved.

## 1. Introduction

The design of shallow foundations on soft clay subject to undrained centric vertical loading is a routine task for the geotechnical engineering profession. To satisfy the ultimate limit state, the designer is required to ensure that applied loads remain remote from the ultimate bearing capacity of the foundation. Design for the serviceability limit state requires that settlement of the foundation under working loads will be small enough to ensure satisfactory performance of the structure it supports. Foundation design therefore requires an ability to predict both the ultimate bearing capacity and settlements under working loads.

As part of the activities of the Australian Research Council (ARC) Centre of Excellence for Geotechnical Science and Engineering (CGSE), an international shallow foundation prediction exercise was conducted with the aim of assessing the predictive capabilities of the geotechnical engineering profession. This paper describes the exercise and compares predictions received from 50 submissions with measured foundation performance of field tests carried out at the Australian National Field Testing Facility (NFTF). It was found that participants significantly overestimated the bearing capacity of the foundation, with the average predicted bearing capacity exceeding the measured value by around 100%. On average, predicted settlement values exceed measured values by more than 600%. To examine reasons for the poor prediction results, a review of strength and stiffness data from the site is presented. It is shown that the site data provides a good indicator of foundation performance via simple foundation models. This suggests that poor

predictions cannot be attributed to inaccurate or insufficient information. An assessment of the sources of over prediction of bearing capacity and settlement is presented and the use of technology to automate the processing of soil data interpretation or development of predictive models that connect directly to soil data are discussed as possible solutions.

## 2. Description of foundation tests

## 2.1. Site description

Supported by the Australian Research Council (ARC), the Centre of Excellence for Geotechnical Science and Engineering (CGSE) established the Australian National Field Testing Facility (NFTF) in Ballina, Northern New South Wales (see Fig. 1). The site is approximately 6.5 Ha and lies on the Richmond River floodplain, located south of Emigrant Creek and west of Fishery Creek.

The ground conditions comprise a crust of alluvial clayey silty sand to a depth of about 1.0–1.5 m, underlain by soft estuarine clay, underlain by a transition zone of clay, silt and sand, then sand of varying thickness [1]. The thickness of the soft estuarine clay increases from approximately 12–22 m from west to east. The engineering geology at the site is described in detail by Bishop [2], Bishop and Fityus [3], Kelly et al. [4]. Fig. 2 shows results from cone penetration tests (CPT) from the site classified using the Robertson [5] soil behaviour index ( $I_c$ ).

## 2.1.1. Geotechnical data

A comprehensive site investigation has been conducted at the NFTF involving drilling and logging over 15 boreholes with high quality soil samples collected and tested in a range of laboratory

\* Corresponding author.

E-mail address: [james.doherty@uwa.edu.au](mailto:james.doherty@uwa.edu.au) (J.P. Doherty).

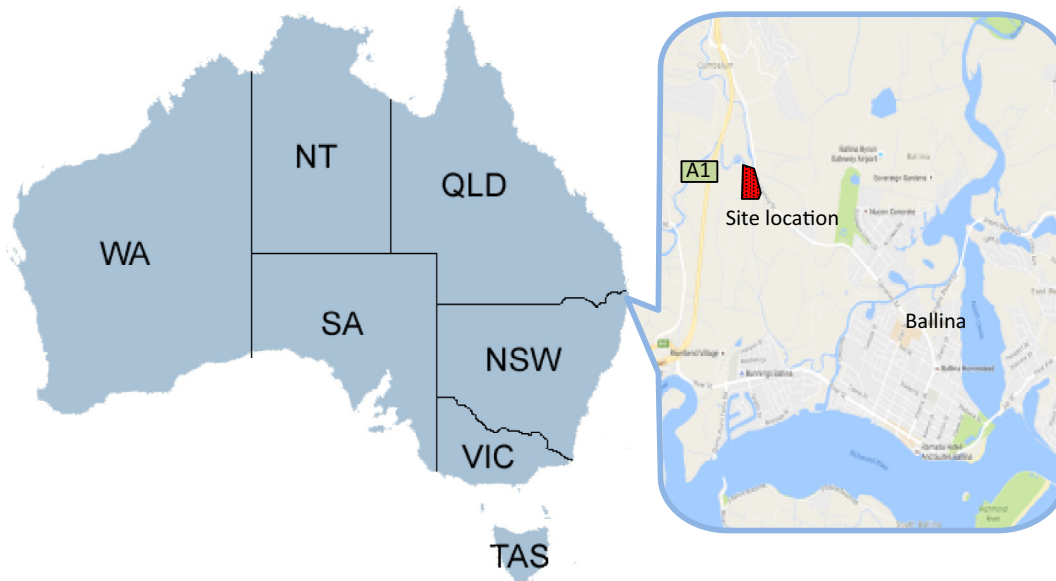


Fig. 1. Location of the Australian National Soft Soil Field Testing Facility (NFTF) at Ballina (NSW).

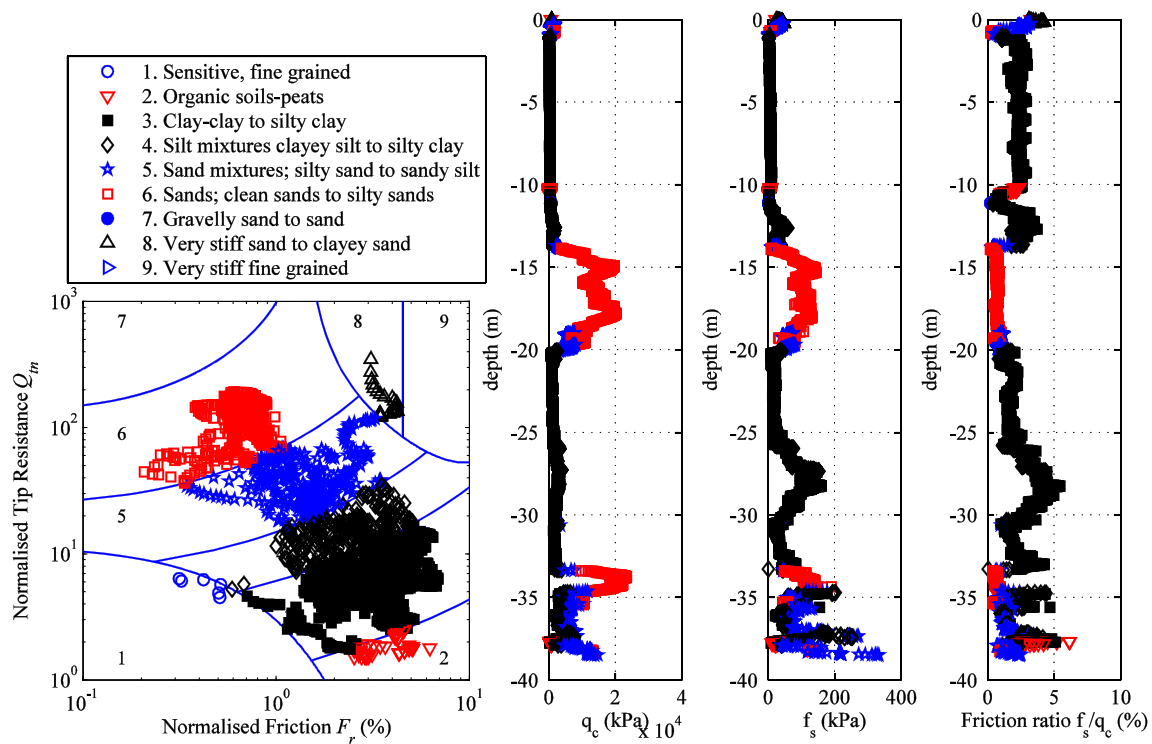


Fig. 2. CPT tests interpreted using *lc* soil behaviour chart.

apparatus [6–8]. A range of in situ tests including cone penetration tests [4,9,10], ball and T-bar penetrometer tests [11] and self-boring pressuremeter tests [12,13] have also been conducted. A web based application (see Fig. 3) was developed to store, manage and publically share all data [14]. Participants in the foundation prediction exercise were able to access the data by registering as a user at [www.geocalcs.com/datamap](http://www.geocalcs.com/datamap), and then using the project registration details given in Table 1. The data will continue to be made freely available on this data sharing platform. Further details can be found in Doherty et al. [14].

### 2.2. Foundation construction and loading details

Two load tests were conducted on almost identical foundations. The foundations, 1.8 m square by 0.6 m high, were constructed in excavated pits 1.5 m deep by 2.4 m square (Fig. 4). Approximately 1 month after construction, the foundations were centrally loaded to failure with precast concrete blocks. Loading of each foundation to failure took approximately 1 h to complete, ensuring undrained conditions. Fig. 5 shows the measured load-settlement response of both foundations. Full details of the field tests are



Fig. 3. Screen shot of datamap web application made available to participants in the foundation prediction exercise.

Table 1  
Project details to access NTF project data.

Project name	NTF
Project code	Ballina

provided by Gaone et al. [15], where Test 1 is referred to as UU1 and Test 2 as UU2.

2.3. Prediction exercise and review of observed and predicted values

The prediction exercise was advertised on the CGSE web site (<http://cgse.edu.au/sfpe2016>) and promoted through social media (LinkedIn and Twitter), the Australia Geomechanics Society and the United States Universities Council on Geotechnical Education

and Research’s (USUCGER) email lists and advertised at a number of conferences. A total of 50 written predictions were received from 88 engineers. Thirteen countries were represented, including Australia, Austria, Belgium, Canada, China, France, Germany, Netherlands, Norway, Japan, Singapore, the UK and the US. Of the 50 predictions, 23 were from industry practitioners, 16 from academics and 11 from undergraduate students.

Participants were invited to make four predictions associated with the foundation performance. These quantities and their measured values are summarised in Table 2 and illustrated in Fig. 5. An ability to accurately predict the ultimate bearing capacity ( $Q_u$ ) is clearly important for ultimate limit state design. For serviceability limit state design, an ability to predict settlements under working loads, which are typically in the range of 25–50% of the ultimate capacity (i.e.  $u_{25}$  and  $u_{50}$ ), is critical. Predicting settlements at 100% of the ultimate load ( $u_{100}$ ) is of less practical importance,

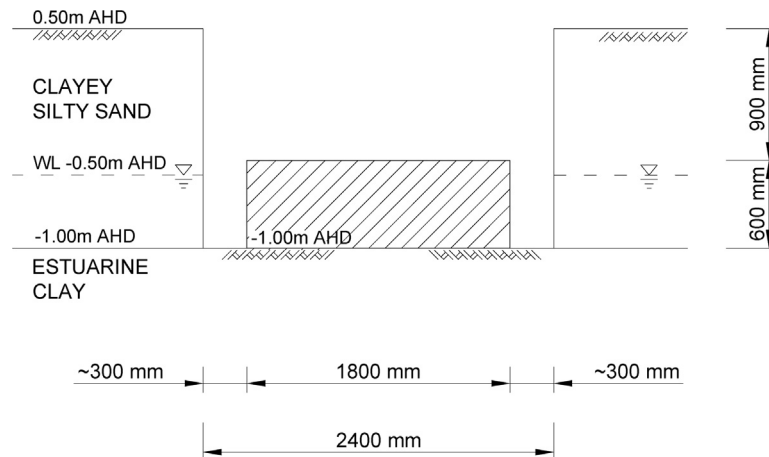


Fig. 4. Foundation geometry.

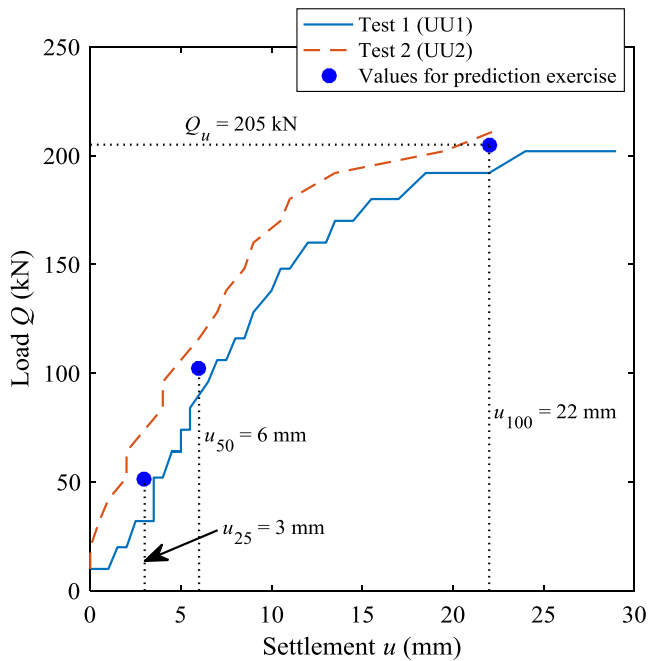


Fig. 5. Measured load-settlement response.

**Table 2**  
Foundation performance values.

Quantity	Measured value
Ultimate failure load $Q_u$ (kN)	205
Settlement at 25% of ultimate failure load $u_{25}$ (mm)	3
Settlement at 50% of ultimate failure load $u_{50}$ (mm)	6
Settlement at 100% of ultimate failure load $u_{100}$ (mm)	22

and clearly more difficult given settlements change significantly with small changes in load. Therefore, less emphasis is placed on interpreting predictions for the  $u_{100}$ .

The predicted values are presented in Table 3 for each performance measure. The error in the predicted values was calculated as

$$\% \text{ error} = 100 \frac{p - m}{m} \quad (1)$$

where  $p$  is the predicted value and  $m$  is the measured value.

Fig. 6 plots the predicted values for each of the four quantities. For each case, predictions have been sorted from smallest to largest and the numbers on the horizontal axis do not correspond to the ID# in Table 3. For each case, the measured and the average predicted values are shown. For the ultimate load (Fig. 6a), the predictions ranged from 130 kN to 2240 kN for a measured foundation capacity of 205 kN. The overall average predicted capacity was 404 kN, which is around 100% greater than the measured capacity. The median prediction was 331 kN, which is 61% greater than the measured value. Fig. 7 presents the cumulative distribution of error for each of the predicted quantities. For the ultimate bearing capacity ( $Q_u$ ) it can be seen that around 10% of participants achieved an error of 20% or less, while 45% achieved an error of 50% or less.

Predictions of the settlement at 25% of the ultimate load ( $u_{25}$ ) are presented in Fig. 6b. The predictions ranged from 0.1 mm to 877 mm for a measured settlement of 3 mm. The overall average predicted  $u_{25}$  was 42 mm and the median value was 8.5 mm. Fig. 7 shows that less than 2% of participants were within 20%, and around 15% were within 50% of the measured value.

Settlement predictions at 50% of the ultimate load ( $u_{50}$ ) are presented in Fig. 6c, which ranged from 0.1 mm to over 1200 mm for a measured settlement of 6 mm. The overall average value was 84 mm, with a median value of 25 mm. Fig. 7 shows that only 22% of predictions were within 100% of the measured value.

Fig. 6d presents the predicted settlements at 100% ( $u_{100}$ ) of the ultimate load, which ranged from 0.8 mm to over 2280 mm for a measured settlement of 22 mm. The overall average value was 275 mm, with a median value of 125 mm. Fig. 7 shows that less than 20% of predictions were within 100% of the measured value.

Fig. 7 shows that the ultimate bearing capacity was more accurately predicted than the settlement. It is noted that if participants made a significant error predicting the bearing capacity, the magnitude of load at which settlement values were predicted are different to the loads at which settlements were measured. This may have contributed to the lower accuracy in the settlement predictions.

Fig. 8 presents the cumulative distribution of absolute error for each of the predicted settlements, since absolute settlement is also significant in geotechnical engineering and the percentage error measure can distort the engineering relevance of the predicted value, particularly for small values of settlement. The cumulative distribution of absolute error indicates that around 65% of participants predicted a settlement that was within 10 mm of the measured  $u_{25}$  and 38% were within 10 mm of the  $u_{50}$ .

Overall, the prediction exercise suggests, at least in the present case, that engineers tend to perceive the bearing capacity of shallow foundations in soft clay to be higher than it actually is, with 82% over predicting the bearing capacity, 55% over predicting by more than 50% and 34% over predicting by more than 100%. The range in values of predicted bearing capacity was more than an order of magnitude (130 kN to more than 2000 kN). Even neglecting the worst 20% of predictions, the range in values of predicted bearing capacity was 130 kN to 480 kN, compared to the measured value of 205 kN.

The prediction exercise also indicates, for the present case, that engineers perceive soil to be less stiff than it actually is, with 88% over predicting the  $u_{50}$ , 76% over predicting by more than 100% and 36% over predicting by more than 500%. It is noted that participants who over predicted the ultimate load were then computing settlements at higher loads.

### 3. A review of undrained shear strength data and its link to measured foundation capacity

Given the participants in the foundation prediction exercise significantly over estimated the foundation capacity - on average by around 100% - this section reviews undrained shear strength data from the site. This data is then used in simple bearing capacity calculations in order to determine if there is a clear and consistent link between the available site investigation data and the measured foundation capacity. Following this, an assessment of the parameter selection and prediction methods for the best and worst predictions is presented.

Using data available to predictors, undrained shear strength profiles may be estimated using a range of in situ and laboratory tests including triaxial compression, triaxial extension [7], shear vane, self-boring pressuremeter [12,13] and cone penetration tests (CPT) [16]. Undrained shear strength profiles derived from each of these data types are plotted against depth below ground level in Fig. 9. For the CPT profile, a ratio of cone tip resistant to undrained shear strength ( $N_{kt}$ ) of 12.2 based on Kelly et al. [1] was used. Ball penetrometer data that was made available after the prediction exercise [11] has also been included in Fig. 9 for completeness. The undrained shear strength was estimated using



**Table 3**  
Predictions for  $Q_u$ ,  $u_{25}$ ,  $u_{50}$ ,  $u_{100}$ .

ID#	Predicted values				% error			
	$Q_u$ (kN)	$u_{25}$ (mm)	$u_{50}$ (mm)	$u_{100}$ (mm)	$Q_u$ (%)	$u_{25}$ (%)	$u_{50}$ (%)	$u_{100}$ (%)
1	690	10	30	500	237	233	400	2173
2	480	8	30	300	134	167	400	1264
3	425	105	145	325	107	3400	2317	1377
4	301	20	38	122	47	567	533	455
5	412	9	18	180	101	200	200	718
6	334	9.5	37.3	382.5	63	217	522	1639
7	280	4	12	120	37	33	100	445
8	437	151	308	371	113	4933	5033	1586
9	300	3	14	50	46	0	133	127
10	1750	13.5	93	1850	754	350	1450	8309
11	286.5	47	94	188	40	1467	1467	755
12	360	8.5	28	206	76	183	367	836
13	513	62	86.8	136.3	150	1967	1347	520
14	222	8.5	21	155	8	183	250	605
15	300	6	12	100	46	100	100	355
16	162	2	7	70	-21	-33	17	218
17	350	10	36	524	71	233	500	2282
18	175	1	3	19	15	-67	-50	-14
19	275	34.5	70.7	203	34	1050	1078	823
20	321	4	12	60	57	33	100	173
21	270	7	15	120	32	133	150	445
22	385	10	19	38	88	233	217	73
23	280	11.5	28	1000	37	283	367	4445
24	162	25	75	180	-21	733	1150	718
25	129.8	7.7	21	176	-37	157	250	700
26	243.5	2	22	60	19	-33	267	173
27	162	380	940	2280	-21	12567	15567	10264
28	373	1.6	1.9	2.4	82	-47	-68	-89
29	580	40	125	300	183	1233	1983	1264
30	412	0.4	0.8	1.4	101	-87	-87	-94
31	2239	877	1256	1742	992	29133	20833	7818
32	200	1.5	6.5	35	-2	-50	8	59
33	600	50	145	375	193	1567	2317	1605
34	600	20	60	300	193	567	900	1264
35	284	5	9	41	39	67	50	86
36	440	5	15	270	115	67	150	1127
37	448	14	27	54	119	367	350	145
38	338	5	11	44	65	67	83	100
39	331	1	4	37	61	-67	-33	68
40	295	27	61	146	44	800	917	564
41	295	31	58	107	44	933	867	386
42	337	5	18	170	64	67	200	673
43	130	6	14	120	-37	100	133	445
44	137	13	26	51	-33	333	333	132
45	427	5.2	40.4	20.9	108	73	573	-5
46	378	3.8	7.6	15.3	84	27	27	-30
47	181.8	0.1	0.1	0.8	-11	-97	-98	-96
48	424	5.2	10.4	20.8	107	73	73	-5
49	413.5	12.6	25.2	50.3	102	320	320	129
50	310	25	51	128	51	733	750	482
Average	404	42	84	275	97	1309	1296	1150
Median	333	9	26	125	62	192	327	468
Standard dev	355	134	218	467	173	4454	3632	2125

a ratio of ball resistance to undrained shear strength ( $N_b$ ) of 14 [17].

The best-fit linear undrained strength profiles were estimated for each test type, as shown in Fig. 9. These profiles were used as input into a Tresca constitutive model in a finite element analysis using the Plaxis finite element software (see Fig. 10). An axisymmetric model was used to simulate the square footing using 15-noded triangular elements. The radius of the foundation and the radius of the excavation were set to give equivalent circular foundation and excavation areas to the field case. The linear undrained shear strength profiles, defined by an undrained shear strength at the foundation base, 1.5 m below ground surface, and a gradient of strength increase with depth, are given in Table 4 for each data type. The computed bearing capacities for each strength profile are also given in Table 4, along with the percentage error compared with the measured capacity. The error ranges

from -26% for triaxial extension to +33% for the vane shear profiles. The triaxial compression, self-boring pressuremeter and ball penetrometer strength profiles gave bearing capacities within 5% of the measured capacity. The CPT strength profile over predicted the capacity by 7%. A parametric study showed that the strength of the crust (see Fig. 10) had negligible impact on the capacity calculations.

Bjerrum [18] derived an empirical factor to correct shear vane strength data to improve predictions of embankment stability in soft clay. Based on a plasticity index for material at the site [7] of around 0.6, the Bjerrum [18] factor would have reduced the vane shear strength profile by around 20%, resulting in a 20% lower bearing capacity calculation and a much better match to the measured bearing capacity. Triaxial extension strengths would typically be expected to result in an under estimate of foundation bearing capacity, as is the case here.

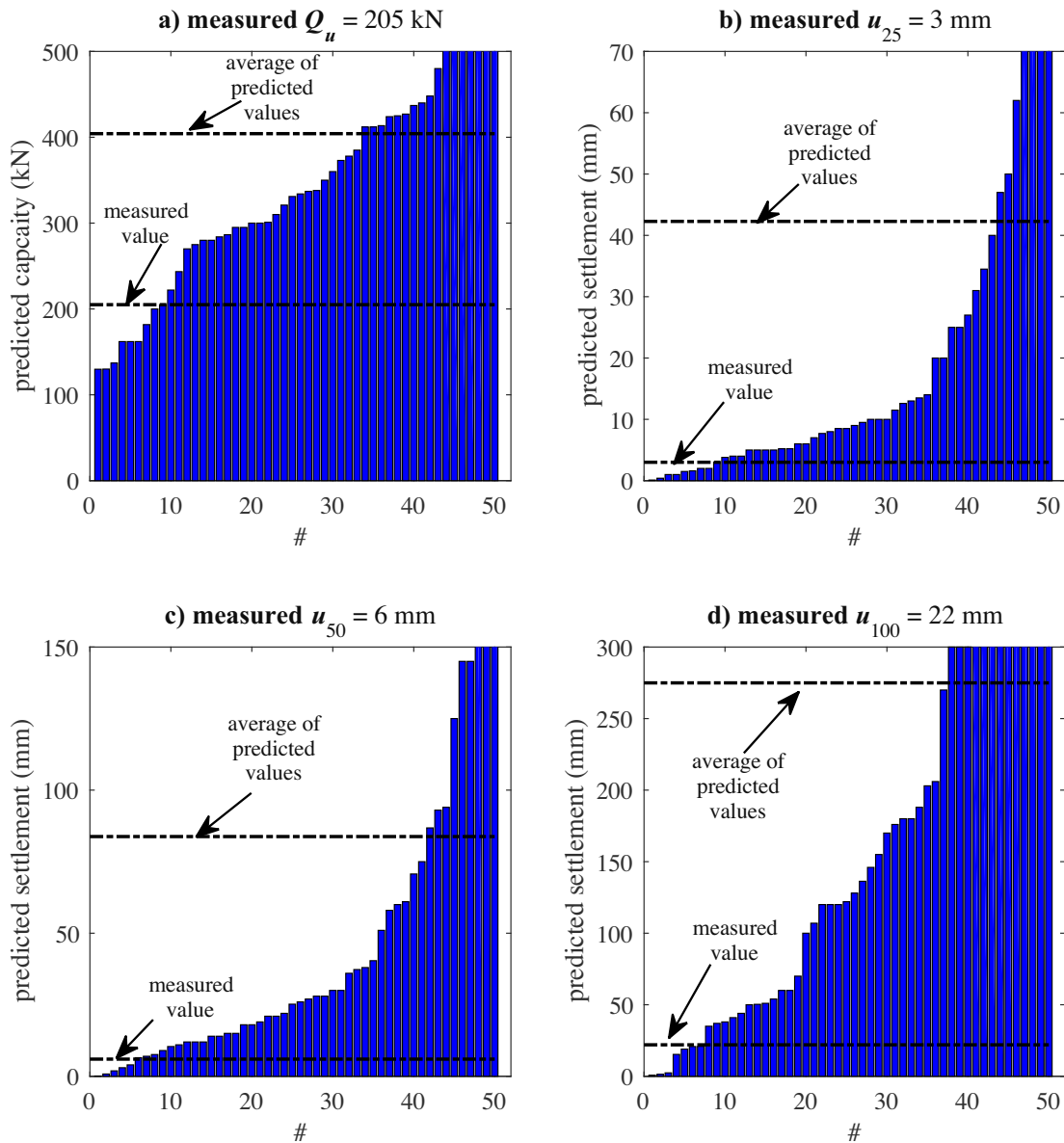


Fig. 6. Comparison of prediction and measured foundation performance for (a)  $Q_u$ ; (b)  $u_{25}$ ; (c)  $u_{50}$  and (d)  $u_{100}$ .

It is noted that changes in undrained shear strength due to excavation of the foundation pit and construction of the foundation were not considered in this analysis. In reality, excavation of the pit to 1.5 m involved a reduction in effective stress of approximately 20 kPa at the foundation base while subsequent construction of the 0.6 m high 1.8 m square foundation involved a re-loading of approximately 10 kPa (assuming a unit weight for concrete of 24 kN/m<sup>3</sup> and noting the position of the water table in Fig. 4).

The analysis outlined here indicates that very reasonable predictions of capacity can be achieved using a simple Tresca soil model with a linear strength profile derived from the data provided. A possible source of error in some predictions may stem from the boundary conditions assumed in the numerical analysis. One issue in particular was that some participants did not model the 300 mm gap between the foundation and the excavation wall (see Figs. 4 and 10), and instead assumed that the excavation wall was immediately adjacent to the foundation (i.e.  $g = 0$  in Fig. 10). To investigate the impact of neglecting the gap, the model was re-run varying the gap dimension  $g$  between 0 and 125 % the value in the axisymmetric model  $g = 0.34$  m. The computed capacity nor-

malised by the capacity with  $g = 0.34$  m is plotted in Fig. 11. It can be seen that in an axisymmetric model, ignoring the gap can influence the bearing capacity by up to around 50%. While the effect of the gap is a potential source for some of the error in predicted capacities, it does not account for the range of error observed, with over half the capacity predictions exceeding the measured value by more than 50%.

It was found that 13 of the 17 participants who over predicted the bearing capacity by more than 100% used simple hand calculations. Out of these 13 predictions, 11 indicated that they had used a bearing capacity calculation of the form

$$Q_u = A(N_c s_u + q N_q) \quad (2)$$

where  $A$  is the area of the foundation,  $N_c$  is the bearing capacity factor,  $s_u$  is the undrained shear strength,  $q$  is surcharge adjacent to the foundation and  $N_q$  is the surcharge factor. By adopting  $N_c = 6$ ,  $N_q = 0$  (due to the gap between the foundation and the excavation wall) and undrained shearing strength values at the foundation level from Table 4, this equation gives very similar bearing capacity esti-

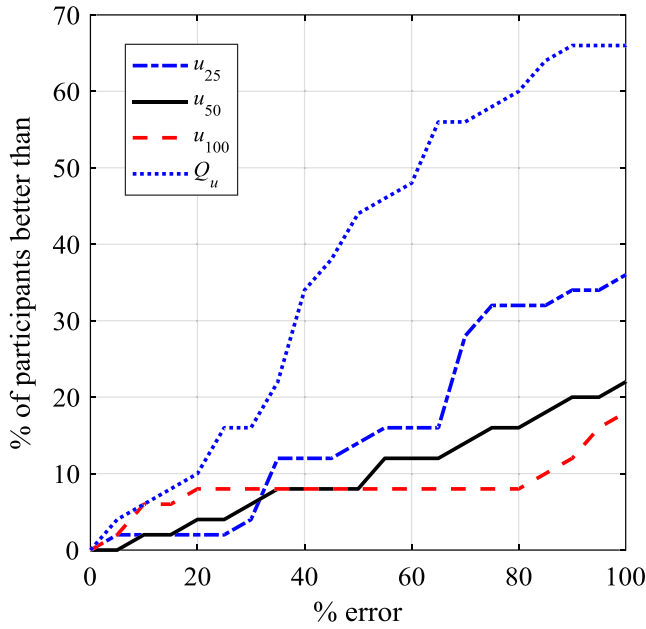


Fig. 7. Cumulative distribution of percentage error for predicted ultimate capacity and settlements.

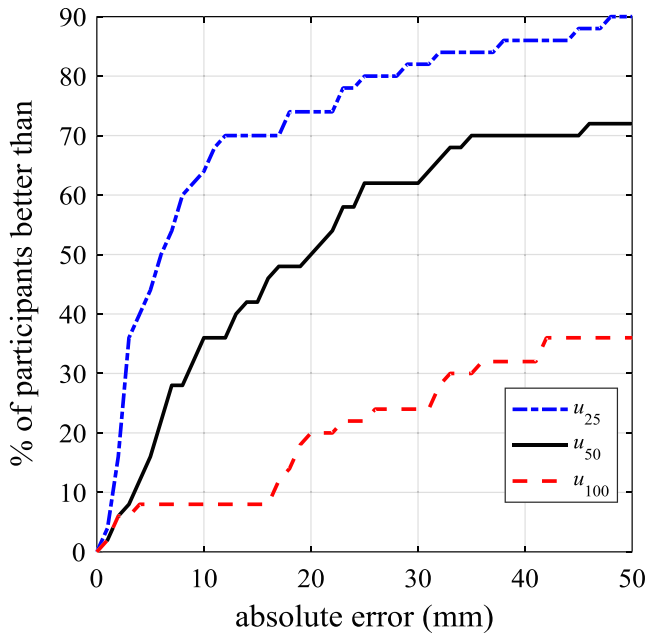


Fig. 8. Cumulative distribution of absolute error for settlement predictions.

mates to those presented in Table 4 from the finite element analysis. It is interesting to note that both the most accurate (ID# 32 in Table 3) and the least accurate (ID# 31 in Table 3) bearing capacity predictions used this equation. The most accurate used  $N_c = 6$  and  $N_q = 0$  along with  $s_u = 10$  kPa in Eq. (2) (and rounded the result up to 200 kN). It was not clear from the submission what factors or undrained shear strength was chosen for the least accurate prediction.

It was found that 4 of the 17 participants who over predicted the bearing capacity by more than 100% used either two or three dimensional finite element analysis, with one using an effective stress method to model undrained behaviour and three using total stress (Tresca) models. Several of the more accurate predictions

also used finite element simulations, with one (ID# 18 in Table 3) using an effective stress approach to simulate undrained behaviour.

Overall, there is no clear trend in terms of which methods worked and which did not. The accuracy appears to be entirely a function of the assumptions made regarding the boundary conditions, soil strength and how model results were interpreted. Clearly, these factors are highly subjective, even for this simple problem.

#### 4. A review of soil stiffness data and its link to measured foundation settlements

This section of the paper focuses on the application of undrained triaxial compression and self-boring pressuremeter data, both of which were available to participants in the foundation prediction exercise, to estimate soil stiffness profiles at the NTF site and examine how these stiffness profiles relate to measured foundation performance.

Stiffness values were estimated from triaxial compression data in three different ways. Using deviatoric stress ( $q$ ) versus axial strain ( $\epsilon_a$ ) data, a point on the curve at 10% of the total change in deviatoric stress mobilised during the compression test was used to compute a secant shear modulus  $G_{10}$ , as shown in Fig. 12a (where the shear modulus is one third of the slope of the secant shown). Similarly, a point on the curve at 50% of the total change in deviatoric stress was used to compute a  $G_{50}$  secant shear modulus (see Fig. 12a). Profiles of  $G_{10}$  and  $G_{50}$  for the site are plotted in Fig. 13a and b, respectively. The third method to derive stiffness values made use of the high quality triaxial compression data by employing a numerical optimisation technique described by Doherty et al. [19] to determine an optimal set of modified Cam clay parameters. The optimised Cam clay parameters were then used to define an elastic shear modulus (inside the Cam clay yield surface). This stiffness value is denoted as  $G_{MCCtx}$ . Fig. 12a shows an example of stress-strain response generated using the modified Cam clay model with optimised parameters. The shear modulus profile obtained using this approach is shown in Fig. 13c.

A shear modulus profile was also derived using a numerical optimisation technique to match the modified Cam clay model to undrained self-boring pressuremeter data. Full details of this process are presented by Gaone et al. [13]. The resulting match of the optimised modified Cam clay model to the pressuremeter data is shown in Fig. 12b. The shear modulus profile  $G_{MCCpm}$  is presented in Fig. 13d.

To estimate foundation settlements using these stiffness profiles, elastic solutions by Doherty and Deeks [20] for circular shallow foundations were used, where the shear modulus varies with depth ( $z$ ) according to

$$G(z) = G_R \left(\frac{z}{R}\right)^\alpha \tag{3}$$

In this equation,  $G_R$  is the shear modulus at a depth equal to the radius of the foundation ( $R$ ) and  $\alpha$  is the non-homogeneity parameter which varies between zero and one, encompassing homogeneous and Gibson soil profiles. Doherty and Deeks [20] presented solutions for circular shallow foundations embedded at the base of an excavation. The solutions were applied by approximating the square foundations as circles with an equivalent area (i.e.  $R = 1.015$  m). Eq. (3) was fitted to each stiffness profile in Fig. 13. The  $G_R$  and  $\alpha$  values for each profile are given in Table 5.

Adopting a Poisson's ratio of 0.5 (for undrained constant volume behaviour), vertical stiffness coefficients ( $K_v$ ) were interpolated from charts presented by Doherty and Deeks [20]. Values for these dimensionless coefficients are presented in Table 5. The foundation settlement ( $u$ ) was then estimated at any load  $Q$  using the following equation

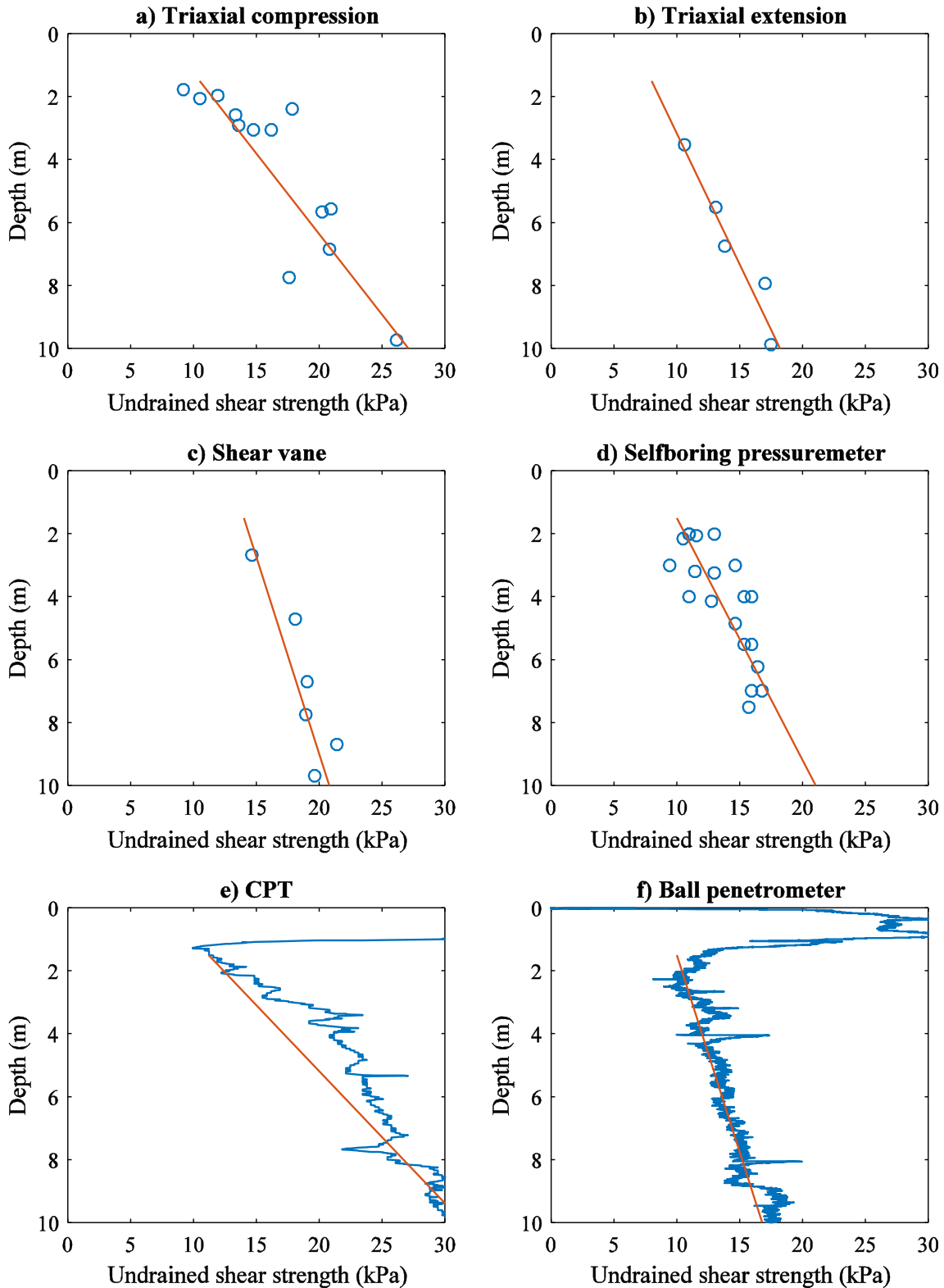


Fig. 9. Undrained shear strength profiles derived from in situ and laboratory tests at the NFTF (a) Triaxial compression; (b) Triaxial extension; (c) Shear vane; (d) Self-boring pressuremeter; (e) Cone penetrometer; (f) Ball penetrometer.

$$u = \frac{Q}{G_R R K_V} \quad (4)$$

Settlement estimates computed at 25%, 50% and 100% of the total failure load,  $Q = 205$  kN, are presented in Table 5.

The elastic load-settlement response for each stiffness profile is presented in Fig. 14 and compared with the foundation performance data. It can be seen that the  $G_{10}$  and  $G_{MCCpm}$  stiffness profiles provide a remarkably good fit to the  $u_{25}$  and  $u_{50}$  settlement values.



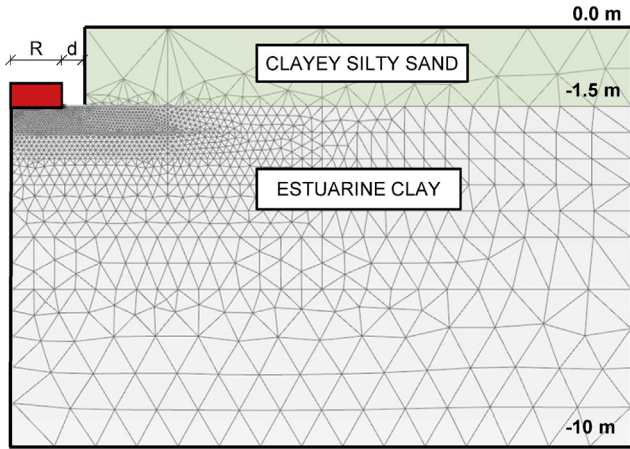


Fig. 10. Axisymmetric finite element model.

The  $G_{MCCx}$  profile also provides a reasonable estimate. Stiffness values derived in this way would therefore be suitable for design of foundations subject to typical working loads. The  $G_{50}$  over predicts foundation settlement at working loads, but provides a reasonable match to the settlements at the onset of failure.

Using the same finite element model described above, a simulation was conducted using a linear-elastic perfectly-plastic Tresca soil model with the  $G_{10}$  elastic shear modulus profile (Fig. 13a and Table 5), a Poisson's ratio of 0.49 and the triaxial compression undrained shear strength profile (see Fig. 9a and Table 4). The resulting non-linear load-displacement response is presented in Fig. 14. It can be seen that this model provides a reasonable match to the measured response, although over predicts the settlement at the onset of failure by around 50%.

Participants in the prediction exercise used a range of methods to predict foundation settlement, including elastic solutions and non-linear finite element analysis. As observed for the bearing capacity predictions, there was no clear trend in terms of method accuracy. This suggests that accuracy was highly dependent on the assumptions made regarding soil stiffness, which is highly subjective. It is interesting to note, that of the 5 predictions that were within 50% of the measured  $u_{50}$ , two based stiffness values on self-boring pressuremeter data. However, some of the poorer predictions also used self-boring pressuremeter data.

5. Concluding remarks

The results from the prediction exercise presented in this paper indicate that engineers with the same data and calculation task judge the data in different ways and ultimately produce very different results. Similar findings have previously been presented for prediction exercises involving shallow foundations on soft clay [21] and for the drained response of shallow foundations on sand [22,23]. This suggests that predictive capabilities have not improved, despite significant progress in modelling and testing techniques in recent years.

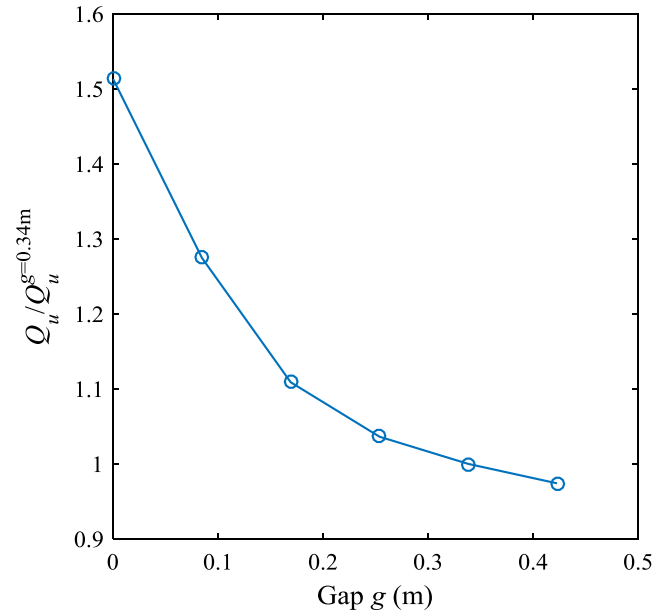


Fig. 11. Impact of the gap,  $g$ , between foundation and excavation wall on calculated bearing capacity.

It was demonstrated that reasonably accurate foundation performance predictions can be achieved using simple foundation models with parameters derived from the in situ and laboratory data provided. Therefore, the poor predictions cannot be attributed to insufficient or inaccurate information. No clear trends could be identified between methods used and the accuracy of predictions for either bearing capacity or settlement. The accuracy appeared to be entirely a function of the assumptions made regarding the boundary conditions, how model results were interpreted and, in particular, how soil parameters were selected. The accuracy of predictions was not strongly correlated to the sector of the predictor (i.e. practitioner, academic or student). The range in the predicted values for both settlement and bearing capacity is undeniably alarming, with settlements varying by more than two orders of magnitude and the bearing capacity by more than one order of magnitude.

A key source of variability in predicted performance stems from the fact that our predictive models (i.e. numerical or analytical methods) remain disconnected from the data that informs them. As a result, significant manual intervention is required to convert in situ or laboratory data into input parameters for use in a predictive model. "Engineering judgement" is applied in this process, which introduces subjectivity and uncertainty in the outcome of design calculations. Automated optimisation tools have been developed to assist engineers in converting measured data from conventional site investigation tests into commonly used constitutive model parameters (e.g. [15,19]), with the aim of reducing this uncertainty. A further step forward involves developing predictive models that connect directly to measured site investigation data. This does not necessarily require machine learning or artificial

Table 4 Undrained shear strength profiles and computed bearing capacities using various laboratory and in situ test data.

	Triaxial comp	Triaxial ext	Shear vane	Self-boring pressuremeter	Cone penetrometer	Ball penetrometer
Shear strength, $s_u$ at foundation level, $z = 1.5$ m (kPa)	10.5	8	14	10	11.2	10
Shear strength gradient, $k_{su}$ (kPa/m)	1.95	1.2	0.8	1.3	2.4	0.8
FEA computed capacity (kN)	207	152	274	194	221	195
% error	+1.2	-25.8	+33	-5.2	+7.2	-4.8

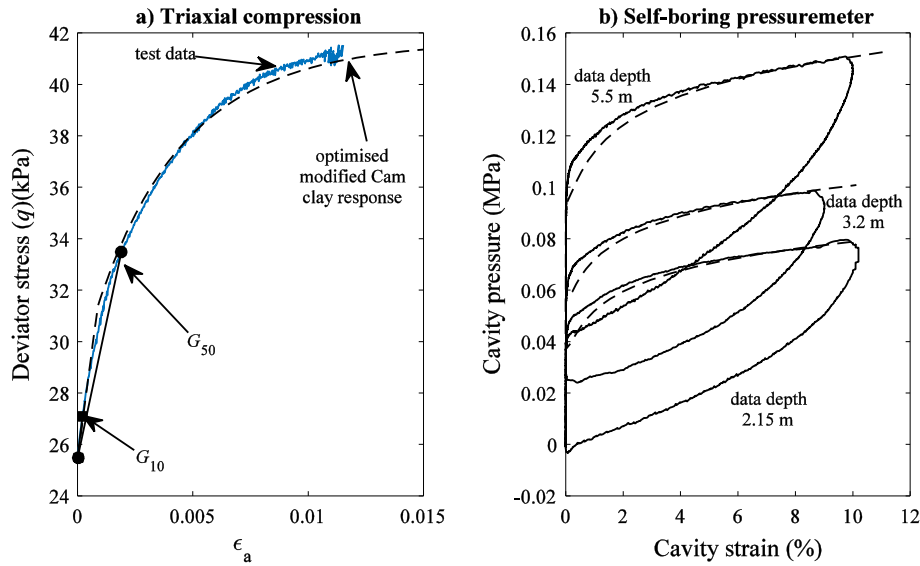


Fig. 12. Stiffness data (a) example stress-strain response from a triaxial compression test with secants at 10% and 50% of the change in deviator stress and optimised Cam clay response; (b) pressuremeter data and optimised modified Cam clay response.

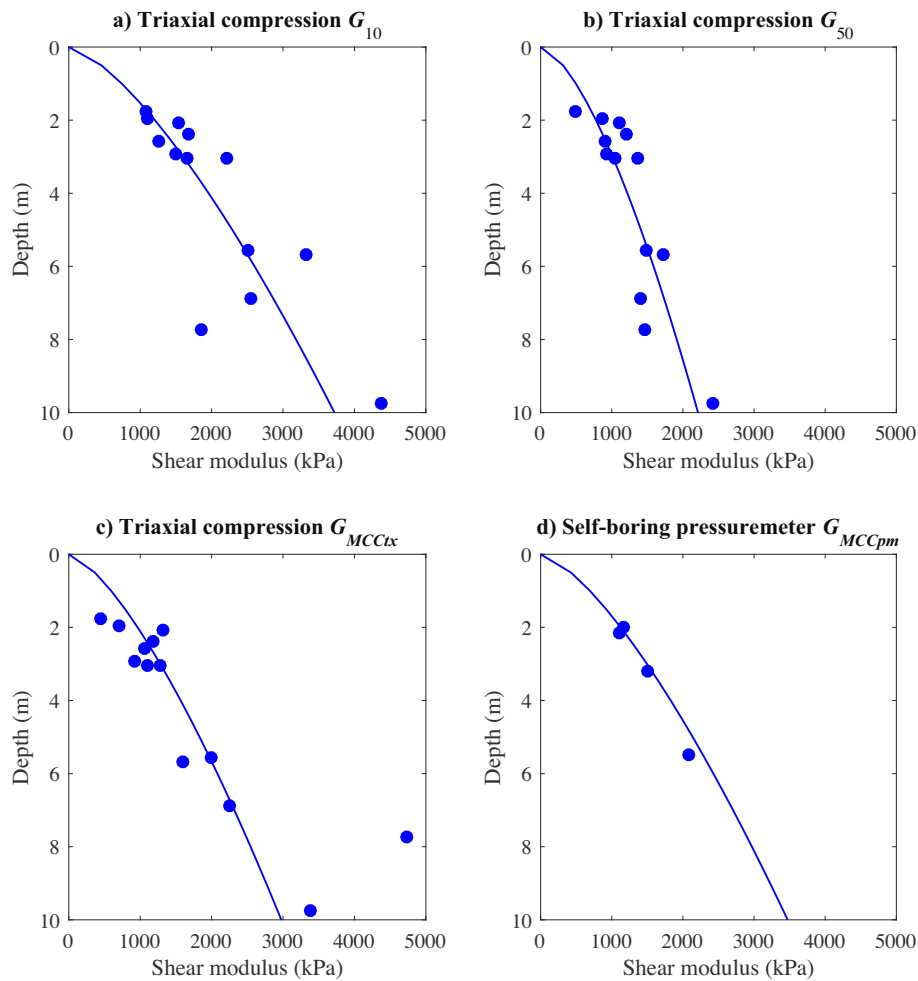


Fig. 13. Shear modulus profiles from triaxial tests and in situ pressuremeter tests at the NTF (a)  $G_{10}$  secant modulus from TXC data; (b)  $G_{50}$  secant modulus from TXC data; (c)  $G_{MCCtx}$  from numerical optimisation of TXC data and (d)  $G_{MCCpm}$  from numerical optimisation of self-boring pressuremeter data.

neural networks, although these methods are options. Doherty and Lehane [24] present an example of this type of integrated analysis that uses CPT or CPTu data directly as an input to perform analysis

of a laterally loaded pile foundation. The application interprets the CPT data and automatically assigns appropriate p-y curves for sands, silts or clays. In principle, the application requires no

**Table 5**  
Stiffness profile parameters, elastic stiffness factors and comparison of predicted settlements with measured data.

	$G_{50}$	$G_{10}$	$G_{MCCtx}$	$G_{MCCpm}$
$G_R$ (kPa)	500	750	600	700
$\alpha$ (-)	0.65	0.7	0.7	0.7
$K_V$ (-)	20.9	22.1	22.1	22.1
$u_{25}$ mm (% error)	4.8 (61.0)	3.0 (1.6)	3.8 (27.0)	3.3 (8.9)
$u_{50}$ mm (% error)	9.7 (61.2)	6.1 (1.7)	7.6 (27.2)	6.5 (9.0)
$u_{100}$ mm (% error)	19.3 (-12.1)	12.2 (-44.5)	15.3 (-30.6)	13.1 (-40.5)

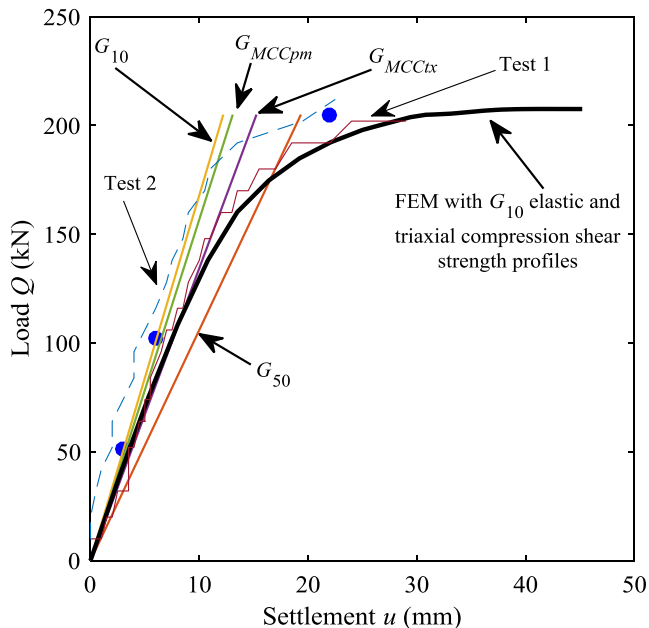


**Fig. 14.** Comparison between elastic load displacement response and measured data for various shear modulus profiles.

engineering judgment to analyse a pile foundation, other than to decide if the CPT data is appropriate for the task. The programme has been deployed as a web based application [25].

By providing large-scale field test data along with extensive high quality in situ and laboratory test data, the Australian National Field Testing Facility provides an invaluable opportunity to calibrate existing and develop new predictive models for classical geotechnical boundary value problems to advance geotechnical knowledge and practice.

### Acknowledgements

This work forms part of the activities of the Centre for Offshore Foundation Systems (COFS), established in 1997 under the Australian Research Council's Special Research Centres Program. Supported as a node of the Australian Research Council's Centre of Excellence for Geotechnical Science and Engineering. The second and third authors and the work presented in this paper are supported through ARC grant CE110001009. This support is gratefully acknowledged.

The authors extend their sincere thanks to all the participants for contributing to this exercise.

### References

[1] Kelly RB, O'Loughlin CD, Bates L, Gourvenec S, Colreavy C, White DJ, et al. In situ testing at the National Soft Soil Field Testing Facility, Ballina, New South Wales. *Aust Geomech* 2014; 50(4)(Special Edition): p. 13–26.

[2] Bishop DT. A proposed geological model and geotechnical properties of a NSW estuarine valley: a case study. In: *Proceedings of the 9th ANZ conference*. New Zealand: Auckland; 2004. p. 261–7.

[3] Bishop DT, Fityus S. The sensitivity framework: behaviour of Richmond River estuarine clays. Australian Geomechanics Society, (Sydney Chapter mini-symposium); 2006. p. 167–78.

[4] Kelly RB, Pineda JA, Bates L, Suwal LP, Fitzallen A. Site characterisation for the Ballina field testing facility 2017;67(4):279–300. <http://dx.doi.org/10.1680/jgeot.15.P.211>.

[5] Robertson PK. Interpretation of cone penetration tests – a unified approach. *Can Geotech J* 2009;46(11):1337–55. <http://dx.doi.org/10.1139/T09-065>.

[6] Pineda JA, Suwal LP, Kelly RB. Sampling and laboratory testing of Ballina clay. *Aust Geomech J* 2014;49(4):29–40.

[7] Pineda JA, Suwal LP, Kelly RB, Bates L, Sloan SW. Characterisation of Ballina clay. *Géotechnique* 2016;66(7):556–77. <http://dx.doi.org/10.1680/jgeot.15.P.181>.

[8] Pineda JA, Liu XF, Sloan SW. Effects of tube sampling in soft clay: a microstructural insight. *Géotechnique* 2016;66(12):969–83. <http://dx.doi.org/10.1680/jgeot.15.P.217>.

[9] Li JH, Huang J, Cassidy MJ, Kelly R. Spatial variability of the soil at the Ballina National Field Test Facility. *Aust Geomech* 2014;49(4):41–8.

[10] Li J, Cassidy MJ, Huang J, Zhang L, Kelly R. Probabilistic identification of soil stratification. *Géotechnique* 2016;66(1):16–26. <http://dx.doi.org/10.1680/jgeot.14.P.242>.

[11] Colreavy C, O'loughlin CD, Randolph MF. Estimating consolidation parameters from field piezoball tests. *Géotechnique* 2016;66(4):333–43. <http://dx.doi.org/10.1680/jgeot.15.P.106>.

[12] Gaone FM, Doherty JP, Gourvenec S. Self-boring pressuremeter tests at the National Field Testing Facility, Ballina NSW. In: *Proc. 5th International Conference on Geotechnical and Geophysical site characterisation, ISC5, Gold Coast, Australia* 2016;1:761–766.

[13] Gaone FM, Doherty JP, Gourvenec S. An optimisation strategy for evaluating modified Cam clay parameters using self-boring pressuremeter test data, submitted for publication.

[14] Doherty JP, Gourvenec S, Gaone FM, Kelly RB, Pineda JA, O'Loughlin C, et al. A novel web based application for storing, managing and sharing geotechnical data, illustrated using the National soft soil field testing facility in Ballina, Australia. *Comput Geotech* 2017;93:3–8.

[15] Gaone FM, Gourvenec S, Doherty JP. Large scale shallow foundation load tests on soft clay – at the National Field Testing Facility (NFTF), Ballina, NSW, Australia. *Comput Geotech* 2017;93:253–268.

[16] Kelly R, Pineda J, Mayne P. In situ and laboratory testing of soft clays. *Aust Geomech J* 2013;48(3):61–72.

[17] Randolph MF, Martin CM, Hu Y. Limiting resistance of a spherical penetrometer in cohesive material. *Géotechnique* 2000;50(5):573–82. <http://dx.doi.org/10.1680/geot.2000.50.5.573>.

[18] Bjerrum L. Embankments on soft ground. Performance of earth and earth-supported structures; 1972. Available at: <<http://cedb.asce.org/CEDBsearch/record.jsp?dockey=0265144>>.

[19] Doherty JP, Alguire H, Muir Wood D. Evaluating modified Cam clay parameters from undrained triaxial compression data using targeted optimization. *Can Geotech J* 2012;49(11):1285–92. <http://dx.doi.org/10.1139/t2012-088>.

[20] Doherty JP, Deeks AJ. Elastic response of circular footings embedded in a non-homogeneous half-space. *Géotechnique* 2003;53(8):703–14. <http://dx.doi.org/10.1680/geot.2003.53.8.703>.

[21] Lehane BM. Vertically loaded shallow foundation on soft clayey silt. *Proc Inst Civil Eng - Geotech Eng* 2003;156(1):17–26.

[22] Lehane B, Doherty JP, Schneider JA. Settlement prediction for footings on sand. In: *4th International symposium on deformation characteristics of geomaterials*. Atlanta, The Netherlands: IOS press; 2008. p. 133–50.

[23] Briaud J-L, Gibbens R. Large scale load tests and database of spread footings on sand. Federal Highway Administration, Report No. FHWA-RD-97; 1997.

[24] Doherty JP, Lehane B. Data driven design – a vision for an automated approach. In: *Proc. 5th International Conference on Geotechnical and Geophysical site characterisation, ISC5, Gold Coast, Australia* 2016;1:1205–1210.

[25] Doherty JP. User manual for LAP, Laterally loaded pile analysis. School of Civil, Environmental & Mining Engineering, University of Western Australia, Perth WA 6009; 2016. Available at <[www.geocalcs.com/lap](http://www.geocalcs.com/lap)>.